

# A Review on Materials and Methods for the Fabrication of Microcavity Laser

Nagesh Bhat<sup>1</sup>, Naveen Kumar J. R.<sup>1,2</sup>, Shrinivasa Mayya D.<sup>2</sup>, Prasad P.<sup>1,2</sup>

<sup>1</sup>Department of Nano Technology, Srinivas Institute of Technology, Mangaluru, Karnataka – 574143, INDIA

<sup>2</sup>Srinivas Centre for Nano Science and Technology, Srinivas University, Mangaluru, Karnataka – 574146, INDIA

E-mail: [hodnanotechsit@gmail.com](mailto:hodnanotechsit@gmail.com)

**Type of the Paper:** Research Review Paper.

**Type of Review:** Peer Reviewed.

**Indexed In:** OpenAIRE.

**DOI:** <https://doi.org/10.5281/zenodo.1404695>.

**Google Scholar Citation:** [IJAEML](#)

## How to Cite this Paper:

Bhat Nagesh, Naveen Kumar J. R., Shrinivasa Mayya, D., & Prasad, P. (2018). A Review on Materials and Methods for the Fabrication of Microcavity Laser. *International Journal of Applied Engineering and Management Letters (IJAEML)*, 2(2), 27-42.

DOI: <https://doi.org/10.5281/zenodo.1404695>.

**International Journal of Applied Engineering and Management Letters(IJAEML)**

A Refereed International Journal of Srinivas University, India.

© With Authors.



This work is licensed under a [Creative Commons Attribution-Non Commercial 4.0 International License](#) subject to proper citation to the publication source of the work.

**Disclaimer:** The scholarly papers as reviewed and published by the Srinivas Publications (S.P.), India are the views and opinions of their respective authors and are not the views or opinions of the S.P. The S.P. disclaims of any harm or loss caused due to the published content to any party.

## A Review on Materials and Methods for the Fabrication of Microcavity Laser

Nagesh Bhat<sup>1</sup>, Naveen Kumar J. R.<sup>1,2</sup>, Shrinivasa Mayya D.<sup>2</sup>, & Prasad P<sup>1,2</sup>.

<sup>1</sup>Department of Nano Technology, Srinivas Institute of Technology, Mangaluru, Karnataka – 574143, INDIA

<sup>2</sup>Srinivas Centre for Nano Science and Technology, Srinivas University, Mangaluru, Karnataka – 574146, INDIA

E-mail: [hodnanotechsit@gmail.com](mailto:hodnanotechsit@gmail.com)

### ABSTRACT

Optical microcavities are resonators that have at least one dimension on the order of a single optical wavelength. These structures enable one to control the optical emission properties of materials placed inside them. One of their most dramatic potential features is threshold-less lasing, unlike the conventional lasers. This is possible due to 2D monolayers, Heterostructures, Hybrid materials which are used as active layers for polariton-exciton strong coupling. In this review paper, a different method of Microcavity laser fabrication is reviewed, where a different type of active materials is utilized to improve the laser efficiency. Materials such as WS<sub>2</sub>, MoS<sub>2</sub>, WSe<sub>2</sub> and MoSe<sub>2</sub> are used due to their strong exciton binding energy. These use high reflecting DBR mirrors fabricated using oxides of a higher refractive index such as SiO<sub>2</sub>, NbO<sub>2</sub>, HfO<sub>2</sub>/Al<sub>2</sub>O<sub>3</sub>, SiO<sub>2</sub>/Ta<sub>2</sub>O<sub>5</sub> and SiO<sub>2</sub>/TiO<sub>2</sub>. In this way, the controlled spontaneous emission is expected to play a vital role in a new generation of optical devices and can have a wide range of applications in Optics, Quantum computing, high-speed signal transmission, etc.

**Keywords:** Microcavity, Photoluminescence, Exfoliation, Quantum Well, Active layer, Q-factor.

### 1. INTRODUCTION :

Einstein pointed out in 1917 that an atom can radiate a photon in two different ways. The first is spontaneous emission, whereby the excited atom spontaneously emits a photon without any influence from outside photons. The other is stimulated emission, in which external photons induce or stimulate the emission of a new photon from the atom. Before the invention of the laser in 1960, only light derived from spontaneous emission process was available for laboratory and home use. After 1960, attention focused on stimulated emission, the essence of laser action [1]. Ultra-short optical pulses of picosecond and femtosecond duration, light sources with a frequency of only a few hertz, and ultrahigh-power lasers producing terawatts are a remarkable example of advanced laser science. These developments are all the result of the coherent laser process in which stimulated emission controlled by a "cavity" dominates the overall process of light emission. However, spontaneous emission has long been widely believed to be uncontrollable. In the last decade, however, marked progress has been achieved in controlling spontaneous emission with the use of wavelength-sized cavities. This research field is now called cavity quantum electrodynamics (cavity QED). Semiconductor microcavity lasers, also called Polariton lasers, are tiny semiconductor lasers with an overall volume in the micrometre regime. Up to now, such miniature lasers have been realized in two fundamentally different configurations. These are the vertical cavity surface emitting lasers (VCSEL) and the micro-disc lasers [2]. A micro-disk laser consists of a disc of semiconductor material with a typical diameter of 2-5 μm, which is thinner than the optical wavelength. Under laser conditions, high-Q whispering gallery modes propagate inside the disc close to the circumference. These modes are confined inside the disc due to the large effective reflection coefficient. The VCSEL has a resonator with very high mirror reflectivity. This high reflectivity is achieved with distributed Bragg reflectors (DBRs), consisting of epitaxially grown layers of different refractive indices. The simplest DBR has

alternating layers that are each  $\lambda/4$  thick to provide constructive interference of the reflected waves from each interface [3].

An optical microcavity is a structure formed by reflecting faces on the two sides of a spacer layer or optical medium. The microcavity is often only a few  $\mu\text{m}$  thick, the spacer layer sometimes even in the nm range. As with conventional lasers, this forms an optical cavity or optical resonator, allowing a standing wave to form inside the spacer layer. The thickness of the spacer layer determines the so-called "cavity-mode", which is the one wavelength that can be transmitted and will be formed as standing wave inside the resonator. Depending on the type and quality of the mirrors, a so-called stop-band will form in the transmission spectrum of the microcavity, a long range of wavelengths, that is reflected and a single one being transmitted. The fundamental difference between a conventional optical cavity and microcavities is the effects that arise from the small dimensions of the system. Quantum effects of the light's electromagnetic field can be observed, and the spontaneous emission rate and behaviour of atoms are altered by a microcavity [1-3]. This generation of light is caused by the formation of Bose-Einstein condensation of Polaritons as polaritons result from strong coupling of electromagnetic waves, an electric or magnetic dipole carrying excitation. This condensate emits spontaneous coherent light waves. Controlling spontaneous emission is also desirable for device applications of particular interest is the concept of a "threshold-less laser." In a conventional laser, only a small portion of the spontaneous emission couples into a single state of the electromagnetic field controlled by the laser cavity, i.e., the cavity resonant mode formed by the cavity mirrors, the rest is lost to free space modes, i.e., it radiates out the side of the laser. This is one of the essential mechanisms behind the occurrence of laser oscillation "threshold" behaviour; full stimulated emission output can be obtained only above a threshold input power that can overcome the spontaneous emission loss to free space modes [4]. The idea of a threshold-less laser is simple. When all spontaneously emitted photons are confined in a cavity whose dimensions are on the order of a single wavelength, loss to the free space mode is eliminated. Then the precise boundary between spontaneous and stimulated emissions inside the cavity is eliminated [5]. To achieve room-temperature operation, the polariton laser diode device is built from the wide-bandgap semiconductor, such as gallium nitride (GaN). The typically large exciton binding energies of such a wideband gap semiconductor make exactions robust at room temperature, which is crucial for practical applications [6].

A new class of few atom thick layered structures called van der Waals heterostructures which are fabricated by structural arrangement of thick atomic layers. These materials can be used with a wide range of materials to utilize them in geometries for optoelectronic devices which allow easy controlling of light-matter coupling. In this work, molybdenum diselenide/hexagonal boron nitride ( $\text{MoSe}_2/\text{hBN}$ ) quantum wells are incorporated in optical microcavities. The strong coupling between  $\text{MoSe}_2$  exactions and cavity photons show part-light-part-matter polariton eigenstates. This provides clear anti-crossing among the neutral exciton and the cavity modes with a 20 meV splitting for a single  $\text{MoSe}_2$  monolayer, which is improved by 29 meV in  $\text{MoSe}_2/\text{hBN}/\text{MoSe}_2$  double-quantum wells. Exciton radiative lifetime of 0.4 ps is obtained due to the splitting at resonance. The results from this work are overlain on the room temperature polaritonic devices based on multiple-quantum-well van der Waals heterostructures, by which polariton condensation and electrical polariton injection through the assimilation of graphene contacts may be realized. By the incorporation of semiconducting transition metal dichalcogenide (TMDC) monolayers, possible applications of Vander Walls heterostructures are investigated [7, 8]. The TMDCs have a direct band gap, such as  $\text{WS}_2$ ,  $\text{MoS}_2$ ,  $\text{WSe}_2$  and  $\text{MoSe}_2$ , demonstrating noticeable exciton resonances at room temperature with excellent exciton binding energies of some 100 meV. The integration of 2D crystal heterostructures enable exciton properties to be manipulated easily [9]. These heterostructures containing single  $\text{MoSe}_2$  monolayers exhibit large Rabi splitting of 20 meV which became 29 meV for a multiple-quantum-well structure with two  $\text{MoSe}_2$  monolayers separated by hBN layer. A radioactive exciton lifetime of 0.4 ps analogous to the homogeneous line width of 1.6 meV is obtained from the coupling strength [10].

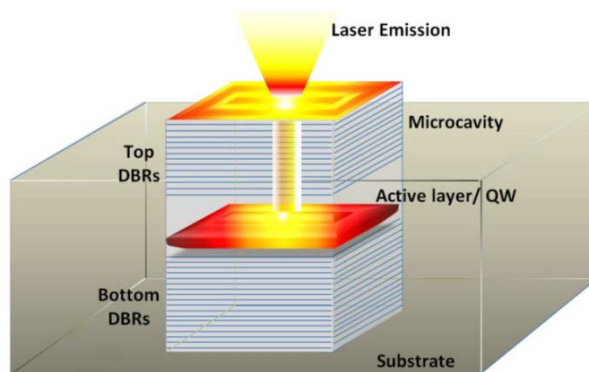


**Fig. 1:** Structure of a VCSEL Microcavity laser

The condensation of the exciton-polaritons in the optical microcavities generates polariton lasers, which are coherent, which arises as a result of the kinetic or thermodynamic regime (Bose-Einstein condensation). The strong coupling of exciton polaritons with part-photon and part-exciton states results in very low threshold operating potential [11]. The conventional lasers require a population inversion mechanism whereas the polariton laser does not require this mechanism because of its Bosonic nature. Based on the higher exciton binding energy and oscillator strength and also the efficient carrier relaxation of the active layer material, the laser can operate at different temperatures. Materials like GaAs [12-15] and CdTe [16] operate at a very low temperature, and the semiconductors with wide band gap are well known for high-temperature operations. Studies revealed that the GaN [17-20] and ZnO [21, 22] active layer lasers well perform at 300 K. The GaN can be doped with both n-type and p-type for good electrical injection made it a material of interest as single defect-free GaN nanowire embedded in an all-dielectric microcavity [23, 24].

The 2D transition metal chalcogenides (TMCs) are viewed after the remarkable study of graphene. These layered crystals of III-IV group such as GaSe, InSe attracted the researchers for the photonic applications as their films of little nanometer thickness possess direct band gap, therefore, allow flexible devices design [25,26]. When the semiconductors are entrenched in the microcavity or waveguides, their light absorption/emission can be increased [27-30]. The semiconductors like MoS<sub>2</sub> and WSe<sub>2</sub> films are coupled to photonic crystal cavities which resulted in enhanced photoluminescence (PL) [31, 32]. Tunable cavity devices are demonstrated with semiconducting thin films sandwiched between the planar distributed Bragg Reflectors (DBRs) [33-36]. In this mirror configuration there seen a possibility for cavity mode confinement in three dimensions with the mode volume of 1.6 μm<sup>3</sup> which is much low. The quality factor of up to 7400 is obtained. Cavity size can be tuned by adjusting the vertical displacement of the two mirrors which results in wavelength tuning over 80 nm by the spectral matching of the cavity mode wavelength by the emitter embedded in the device. With the monolayer of MoS<sub>2</sub> and few layers of GaSe and by moving the top mirror out of the optical path, the emission spectra and the intensity of strong peak PL can be highly modified [37]. The ability of TDMCs to produce large and atomically thin monolayers with abundant exciton-binding energy made them use widely in optical devices [38-43]. Their optical properties provide stable exciton formation at room temperature, narrow absorption peaks and high photoluminescence quantum yields [44-48].

A single atomic layer of direct band gap WS<sub>2</sub> of 0.8 nm thick interacts with light strongly that it has an absorbance of 0.1 and shows strong PL [45]. WS<sub>2</sub> is suitable for room temperature applications as it has large exciton binding energy of ~ 0.7 eV. WS<sub>2</sub> is used in open microcavity with cavity setup such that in-situ tunability of coupling strength between the optical mode and WS<sub>2</sub> excitons is possible [49]. This showed strong coupling in a monolithic microcavity, but the resolution of spectra with splitting's below the exciton line width is unwell [50, 51]. The transversely confined microcavities at low temperatures let the creation of polaritons in MoSe<sub>2</sub> with Rabi splitting of 70 meV. This exceeds exciton line width, permitting in-situ variability of the coupling strength [52]. The photonic crystal cavity light emitters work on the principle of Quantum electron dynamics which considerably increases the spontaneous emission rate in the Purcell regime. The reduction of the lasing threshold of

emitters due to this effect provides low threshold lasing action with low power consumption, small footprint and ultrafast modulation [53-57].

Photonic Crystal cavities (PCC) [58-60] consisting of Quantum dots (QD) [59] in them creates an ultralow-threshold nanoscale laser. The random positions and compositional fluctuations of the dots, extreme difficulty in current injection, and lack of compatibility with electronic circuits remain as some of the problems. Anatomically thin crystalline semiconductor  $WSe_2$  is used as a gain medium at the surface of a pre-fabricated PCC. An optical pumping threshold as low as 27 nanowatts at 30 K temperature, as seen in the QD/PCC lasers, emits a visible regime continuous laser [59]. This depends on the confinement of direct bandgap excitons by the monolayer of gain media at the PCC surface and its nature. This surface gain geometry provides excellent accessibility and tailorability of gain properties through external electrostatic gating and current injection which makes more comfortable electrical pumping. The TDMCs are semiconductors with a direct bandgap in the visible frequency range, having chemical formula  $MX_2$ , due to the tight exciton bonding [60-65]. These materials are used in many applications such as spintronics [66, 67], FET [68], LEDs [69-71], solar cells [72] and in photodetectors [73] with their excellent properties being strong, stable, tunable and optically active. In this work, the demonstrated design is possibly scalable nanolaser which uses 2D monolayers which can be used in the integrated chip systems. This surface structure provides an advantage of easy optical nanocavity construction such that the main material can be separated from the cavity and the parts are individually fabricated with high quality, non-destructive hybrids [74].

## 2. PREPARATION OF 2D FILMS FOR MICROCAVITY LASERS :

### 2.1. Preparation of $MoSe_2$ and hBN films:

The 2D film fabrication for the microcavity laser follows thin film formation mechanical exfoliation of  $MoSe_2$  and the hBN. These thin films are then transferred one over another to form a 3 nm thick, thin film and finally this stake of the layer is transferred using standard transfer methods on to a dielectric mirror which is fabricated in the next step.

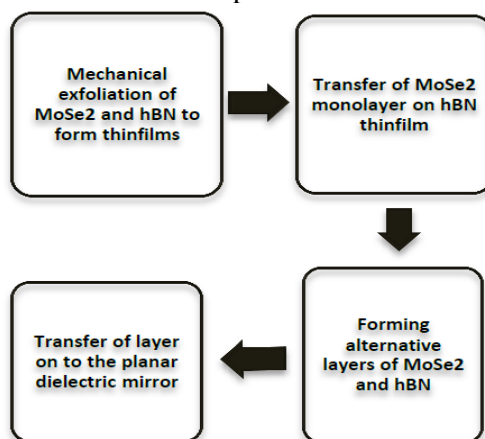


Fig. 2: Steps indicating  $MoSe_2$  and hBN layer preparation

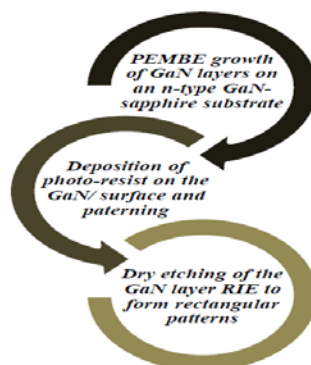


Fig. 3: Steps for Growth of GaN layers

**2.2. The growth of the GaN layer on a substrate:**

Here in this study the film is directly grown on the substrate instead of growing it separately and transferring on to the mirror. The GaN microcavity fabrication involves growth and etching techniques which include Plasma Enhanced Molecular Beam Epitaxy (PEMBE), Photolithography, Reactive Ion Etching (RIE) (dry etching), photochemical etching (PCE) and Atomic Layer Deposition (ALD). First, the GaN layer is grown by PEMBE on the n-type GaN-sapphire substrate and is patterned using photoresist. The rectangular pattern is etched by RIE, and then the photo-resist is removed by photochemical etching.

**2.3. Exfoliation of MoS<sub>2</sub> and GaSe layers:**

The layers of MoS<sub>2</sub> and GaSe layers are cleaved mechanically using exfoliation tape. The GaSe layer is directly transferred on to the substrate. The MoS<sub>2</sub> layer is transferred on to the polymer layer, i.e. PMMA, which is then, transferred using a specific transfer technique.

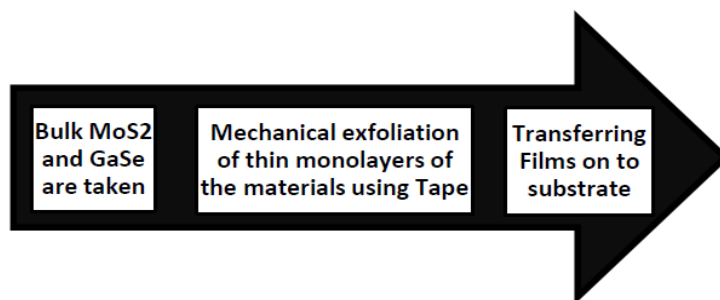


Fig. 4: MoS<sub>2</sub> and GaSe exfoliation steps

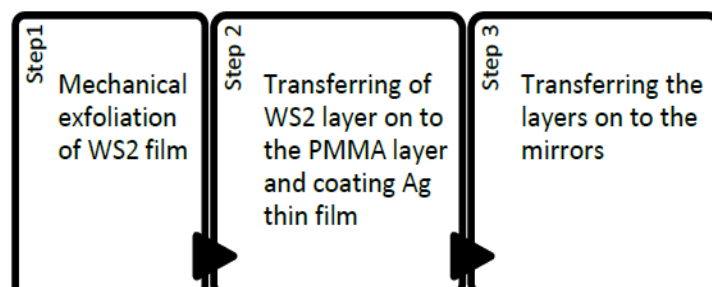


Fig. 5: Steps to synthesize WS<sub>2</sub> flakes

**2.4. Synthesis of triangular WS<sub>2</sub> flakes:**

In this study, WS<sub>2</sub> flakes (layers) are synthesized by the mechanical exfoliation method which is obtained more likely in a triangular shape. The transferring of these flakes on to the DBR mirror uses PMMA polymer layer as like in the previous study. The PMMA layer used to transfer the WS<sub>2</sub> layer. After transferring the layers, PMMA is washed out.

**2.5. Preparation of WSe<sub>2</sub> films:**

The whole laser cavity structure is fabricated by hybridizing the PCC, which is fabricated separately, with WSe<sub>2</sub>. This PCC- WSe<sub>2</sub> hybrid structure is produced by a polymeric-transfer method where the mechanically exfoliated WSe<sub>2</sub> layer is first transferred on to the polymer coated silicon substrate. Silicon substrate is spin coated with polyvinyl alcohol (PVA, 1%) and then coated with poly (methyl methacrylate) (PMMA, 6%). The exfoliated WSe<sub>2</sub> layer is placed on this polymer coated substrate and is placed in water. The PVA dissolves in water, and WSe<sub>2</sub>/PMMA layer gets separate from the Si substrate, which is then transferred on to the PCC surface. Then the PCC is heated and placed in acetone and isopropyl alcohol bath to dissolve the PMMA, leaving the WSe<sub>2</sub> layer on top of the PCC.

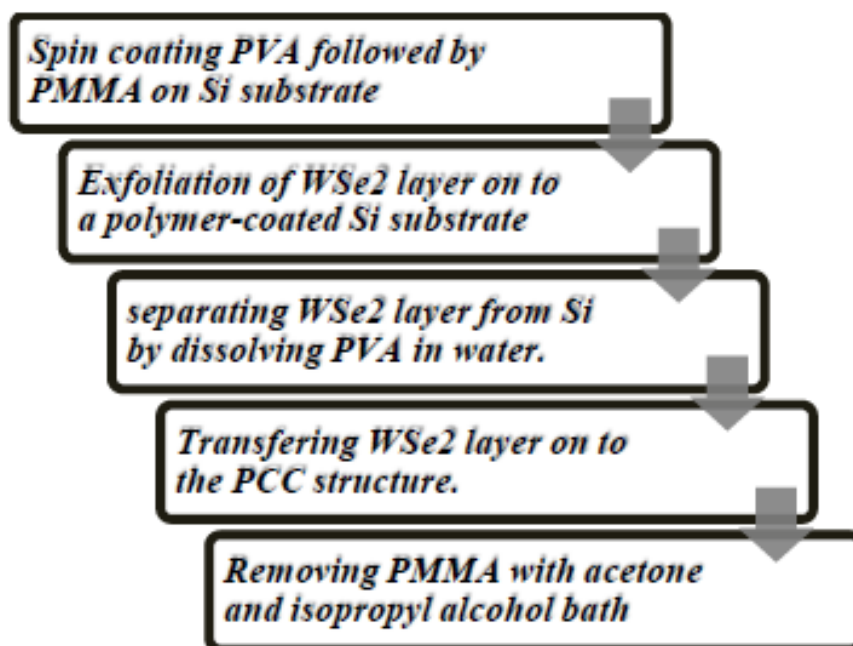


Fig. 6: Flowchart for forming WSe<sub>2</sub> films

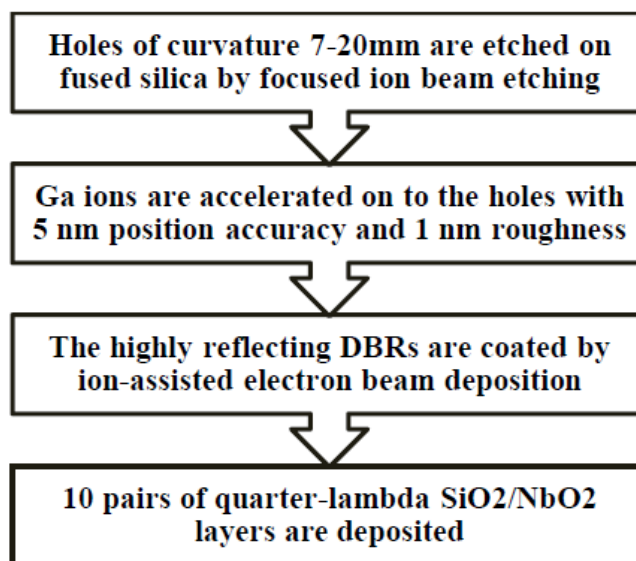


Fig. 7: Flowchart for hBN/ MoSe<sub>2</sub> microcavity fabrication

### 3. MICROCAVITY LASER DEVICE FABRICATION :

#### 3.1. Fabrication of microcavity using fused silicon/Ga substrate and incorporation of hBN/ MoSe<sub>2</sub>:

The dielectric mirror of the laser is fabricated mainly in four steps. The microcavity of 7-20 nm is etched out of the substrate, i.e. fused silicon substrate by focused ion beam etching. The semiconducting mirror is formed by the depositing Ga atoms inside the hole with position accuracy and roughness of 5 nm and 1 nm, respectively. Over this layer, several alternate layers of SiO<sub>2</sub> and NbO<sub>2</sub> is coated by an ion-assisted electron beam deposition method, which forms large reflective DBRs mirrors in the cavity. These mirrors are deposited for the centre wavelength of 750 nm with stop bandwidth of 200 nm. The prepared 2D films of hBN and MoSe<sub>2</sub> is then transferred on to the

dielectric mirror to complete the Microcavity laser fabrication.

After the fabrication the device is optically measured using picosecond-pulsed, frequency doubled titanium–sapphire laser with a pulse length of around 3 ps for time-resolved measurement. PL from the device is analyzed using a 0.75-m spectrometer and a high sensitivity charge-coupled device for emission collection [10].

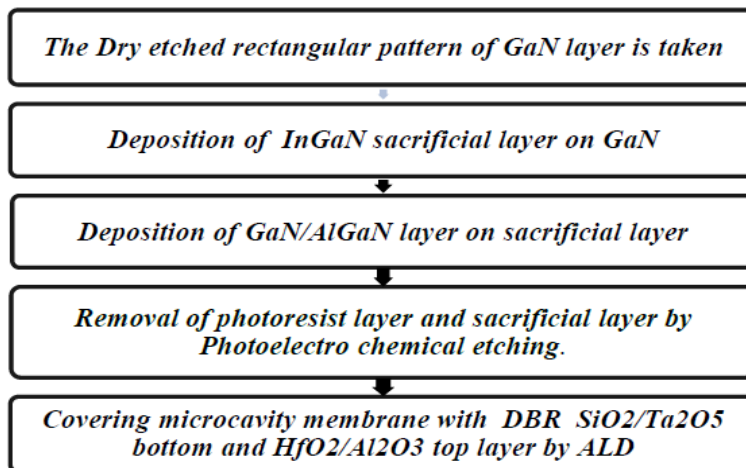


Fig. 8: Stepwise fabrication of GaN/AlGaN layer microcavity

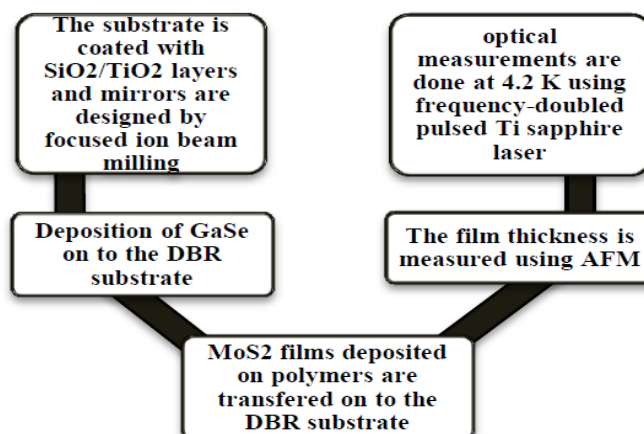


Figure 9: Steps in MoS<sub>2</sub>/ GaSe layer microcavity fabrication

### 3.2. Fabrication of GaN/AlGaN layer microcavity:

The patterned layer grown on the substrate is then undergone through several steps to fabricate the microcavity device. The sacrificial layer InGaN is deposited by PEMBE, and GaN/AlGaN layer is deposited over the sacrificial layer. The sides of the sacrificial layers are etched out by PCE. Finally, the microcavity is sealed with pairs of top DBR layers of HfO<sub>2</sub>/Al<sub>2</sub>O<sub>3</sub> and bottom DBR layer SiO<sub>2</sub>/Ta<sub>2</sub>O<sub>5</sub>, which are deposited using the ALD technique.

### 3.3. Formation of MoS<sub>2</sub>/ GaSe layer microcavity:

In this method, the substrate on which microcavities are being developed at first coated with SiO<sub>2</sub>/TiO<sub>2</sub> layers, and the concave mirrors are designed by focused ion beam milling. The thin films of MoS<sub>2</sub> and GaSe which in the early step exfoliated mechanically, which are of a thickness in the range of 30-100 nm are transferred on to the mirrors. The GaSe layer is directly transferred on to the DBR substrate, and the MoS<sub>2</sub> layer is deposited on a polymer, then moved on to the DBR by a specific transfer technique. With the help of AFM (Atomic Force Microscopy), proper arrangement and thickness of transferred layers are confirmed. This system has undergone optical measurements using frequency doubled pulsed Ti-sapphire laser at 4.2 K temperature.

**3.4. Fabrication of WS<sub>2</sub> layer based microcavity:**

In this study, the open microcavity is fabricated using DBRs of several pairs of mirrors made of SiO<sub>2</sub>/TiO<sub>2</sub>. The central wavelength of these mirrors is 637 nm. SiO<sub>2</sub>/TiO<sub>2</sub> DBR layers are deposited on to the substrate with 50 nm thick silver mirror, which is deposited by a thermal evaporation method. The exfoliated or grown WS<sub>2</sub> flakes is transferred on to the DBR layer through a transfer method using PMMA polymer sheet as a helper layer for transfer mechanism. After transfer and etching processes and heating the layer up to 150°C, the PMMA layer is removed by its dissolution in an acetone bath. The thin silver layer helps in the controlling of cavity length. The device is analyzed using And or combined spectrometer/CCD system.

**3.5. AlGaP/GaP photonic crystal cavity (PCC) fabrication:**

The Photonic Crystal Cavity (PCC) is fabricated using AlGaP and GaP semiconductors. GaP wafer is taken as a substrate, and the AlGaP layer is coated on to it by Gas Source Molecular Beam epitaxy (GSMBE). A layer of GaP is again deposited on to the AlGaP layer. The ZEP520 photoresist is coated on to the GaP and patterned with Electron Beam Lithography (EBL). This pattern is then transferred on to the GaP by Chlorine based-RIE. Later on, the resist is removed, and the sacrificial layer is one undercut by Hydrogen Fluoride (HF) solution. Finally, the fabricated PCC is cleaned with KOH to remove etched material or the unwanted by-product.

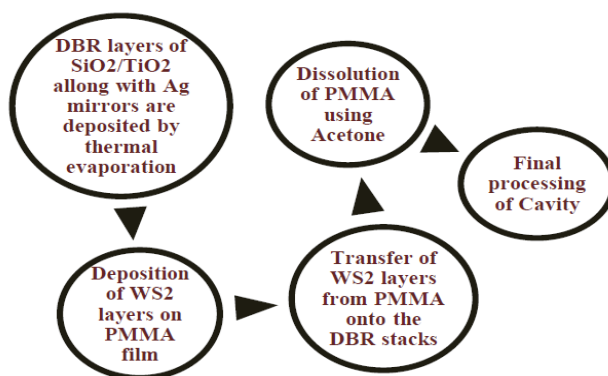


**Fig. 10:** Flowchart for WS<sub>2</sub> layer based microcavity device fabrication

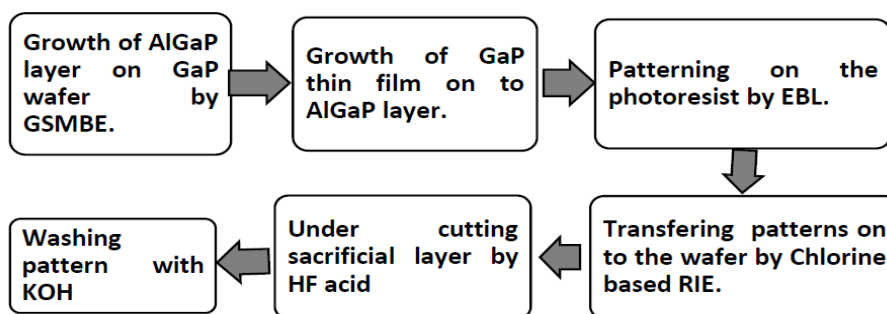


**Fig. 11:** Photonic Crystal Cavity (PCC) fabrication

**4. EFFICIENCY OF hBN/ MoSe<sub>2</sub> INCORPORATED FUSED SILICON/Ga MICROCAVITY LASERS :**

The device design by S. Dufferwiel et al. [10] provides excellent control over mirror separation through which independent positioning of the two DBRs and the cavity mode resonances can be tuned in-situ. The cavity made of heterostructures consists of three parts: single Quantum well (QW), double QW and a bilayer MoSe<sub>2</sub> region. Single monolayer sheet of MoSe<sub>2</sub> 3-nm-thick sheet of hBN makes the single QW. The spectrum contains a neutral exciton and a negative ion with a line width of 11 meV and 15 meV respectively. The spatial positioning of the two independent mirrors can be possible with open cavity system. The cavity consists of a monolayer of MoSe<sub>2</sub> as an active region

with a concave mirror of radius of curvature 20 mm. The longitudinal resonance is at 1.588 eV at  $V=0$  with modes at higher energy are its associated first 1.608 eV and second 1.628 eV transverse modes. The total optical cavity length is around 2.3 mm and the longitudinal mode number  $q=5$ . Rabi splitting of 20 meV for a single  $\text{MoSe}_2$  monolayer is observed in the longitudinal mode which is by the theoretical value of 26.7 meV. The PL spectra are seen in the detuning range of 16-12 meV, and the upper polariton branch (UPB) at positive 40 meV and lower polariton branch (LPB) at negative 30-20 meV are observed. The polariton peak energy results in an increase in the Rabi splitting of about 29 meV with the multiple QW-TDMC heterostructures. Radiative lifetime of 0.4 ps for exciton at a similar line width of 1.6 meV is obtained with coupling strength of 8.2 meV.

### 5. GaN/AlGaN LAYER MICROCAVITY LASERS :

The study by R. Jayaprakash et al. [25] shows that the LPB discrete, strong coupling at large angles at 20 K and flattens due to cavity mode interaction with QW excitons and LPB dispersion redshift with temperature and the UPB are not seen. At 230 K additional branches for large angles were distinguished called Middle Polariton Branch (MPB) due to photon coupling with the excitons located at the 25 nm GaN spacer. MPB is also visible in negative detuning at 80 K, and 300 K as a result of uncoupled exciton intensity loss, the dispersive nature of the MPB and its anti-crossing with the LPB can be more seen. Increasing temperature also tends to increase LPB line width. For the room temperature PL at the angle of  $10^\circ$  from the membrane, the spectrum shows LPB narrow line at 3.402 eV with a linewidth of 10.8 meV and a weaker MPB for uncoupled QW exciton at 3.453 eV. To find the quality factor, the absorption spectrum is estimated at the  $10^\circ$  incident angle by a transfer matrix model, which is then utilized in extracting the PL data considering the proportionality between absorption and spontaneous emission. The QW and GaN spacer excitons are defined at 3.453 eV and 3.422 eV respectively with a similar line width of 28 meV at 300 K. The lasing action starts with a minimal midrange power density of 4.5 W/cm<sup>2</sup>, and this power is four times less in comparison with GaN QW microcavities. It is noted that the occupation increases with power linearly at below threshold powers and also at large angles. Also, the blue shift of the LPB is absent until the threshold. Compared to the conventional lasers the exciton saturation density is less by order of magnitude by 2.5 and 3.5 times less electron-hole pair densities needed for population inversion. These results are due to the zero-dimensional confinement and optical quality of the structure of the material used.

### 6. MoS<sub>2</sub>/ GaSe LAYER MICROCAVITY LASER EMISSION RESULTS :

$\text{MoS}_2$  monolayer shows PL in a wide range of 640-740 nm and GaSe film of thickness 43 nm emission is seen in the range 600-625 nm from localized exciton state due to the interlayer stacking defects. The cavity formed such that the mirror placed above the optical excitation area along with top DBR. This study conducted by S. Schwarz et al. [38] displays the quality factor of cavity mode coupled with the PL is about 103 and that of the mirror about 7400. The emission is expected from a spot in the cavity for which the diameter of the spot is 7 and 1  $\mu\text{m}$  for half and full cavity configuration respectively. It is observed that the excitation density for the 2D film is 6.5 kW/cm<sup>2</sup> and strongest peak for longitudinal mode is around 675-680 nm for which the Q-factors in the spectra are 4000, 3000, 1800. For the concave top mirror with a radius of curvature  $R_c$  16, 10 and 5.6  $\mu\text{m}$  the PL intensity increased by 10, 30 and 60 times respectively than the  $\text{MoS}_2$  monolayer. From this one can tell that by adjusting the distance between the mirrors, in turn, the cavity length and cavity resonance frequency can be tuned and the tuning is restricted by the size of stop band which is  $\sim 200$  nm in this case. The modes near GaSe emission window can also be tuned up to  $\sim 600$  nm, and the time-resolved PL measurement straightly provides possibilities for Purcell enhancements by relating the radiative lifetimes with and without the effect of the cavity. PL saturation is reached at  $P \sim 10$  mW which shows that the optical pumping rate surpasses the relatively low recombination rate. By this, it is clear that the carrier radiative lifetime is shorter in the case when the full cavity is designed, the effect calculated with the 10-fold PL decay time shortening.

### 7. WS<sub>2</sub> LAYER BASED MICROCAVITY TEST RESULTS :

The  $\text{WS}_2$  films grown by CVD are moved on to the low-index terminated distributed Bragg reflector

(DBR) using a PMMA transfer layer. For different cavity lengths following the mode with longitudinal mode number  $q = 3$ , the transmission spectra are assimilated in succession. Linear feedback in cavity mode energy affecting from 1.85 eV to 2.15 eV is due to decrease in the cavity length from 260-130 nm. At 2.01 eV  $WS_2$ , monolayer exciton energy remains constant. The Rabi splitting obtained is about  $(70 \pm 2)$  meV, and the UPB and LPB are found to be lesser than Rabi splitting those are  $(55 \pm 7)$  and  $(34 \pm 5)$  meV respectively. The edge of the stop-band of the DBR which is centred nearby 1.95 eV results in increasing Cavity mode line width from  $\approx 30$  meV to  $\approx 60$  meV. As the LPB energy nears the exciton energy, LPB gets populated gradually and attains maximum for  $15 \text{ meV} < \Delta E < 30 \text{ meV}$  and drops quickly for  $\Delta E \rightarrow 0$ . The total polariton population differs for distinct longitudinal cavity modes, decreases as the Rabi splitting becomes smaller. A bath of the exciton is created due to the high excitation in the conduction band of the  $WS_2$  monolayer which causes population in the LPB later on. The generation of exciton-polaritons takes place with coherent interchange of energies of excitons and polaritons at the Rabi splitting of  $70 \pm 3$  meV in a vacuum in this experiment which is conducted by the L. C. Flatten et al. [53].

### 8. AIGaP/GaP PHOTONIC CRYSTAL CAVITY (PCC) STUDIES :

Semiconductor monolayers are used in Low Q-factor PCC or DBRs by Sanfeng Wu et al. [75], which show controlled spontaneous emission. These PCCs are of high Q-factor of 104, which is 30 times that of conventional PCC. The thin membrane of few nm offers high Q-cavity in the visible region. 40% of the allowable maximum electric-field intensity at the monolayer and this allows useful intersection of cavity mode and the monolayer  $WSe_2$  on the surface. At 80 K, under optical pumping of 632 nm continuous laser, a typical laser emission spectrum can be obtained by the hybrid structure, where the sharp feature can be seen at 739.7 nm. A line width of 0.3 nm at the half-maximum is measured on the spectrum and emission power of 10 fW for 100 nW input power. These fabricated cavities are of Q-factor in the range of 5000 to 14000 which gets reduced from 8000 to 1300 upon monolayer transfer and again gains Q-factor of 2500 while cooled to cryogenic temperatures. The Q-factor and resonance shift, due to the PMMA layer, becomes 500 and 750.7 nm respectively. This shows that high Q-factor enhances the spontaneous emission rate in lasing mode and ultralow threshold lasing.

### 9. CONCLUSION :

The 2D heterostructures demonstrate a robust exciton-photon coupling in microcavities with tunable PL and reflectivity. The room temperature operation of these heterostructures devices is possible as they present high flexibility with graphene contacts to supply current. In comparison with the existing semiconductor materials, namely GaAs, GaN and ZnO, VDW heterostructures show fine tuning and seem to be of promising technological attention. A room temperature, ultralow threshold, all-dielectric, high-Q QW microcavity polariton laser with spontaneous zero-dimensional confinement is revealed. Studies showed enhancement of characteristics of polariton laser with 0D confinement along with the new materials and right optical property of the structure and a new outgrowth in the field of laser optics, especially in room temperature polaritonics. Also, tunable dielectric 2D film metal-chalcogenides microcavity fabrication is demonstrated where photonic fields are localized in the entire three dimensions, and the PL spectral properties are altered strongly by the cavity. The microcavity with  $MoS_2$ , GaSe,  $MoSe_2$ , and  $WS_2$  inside shows increased cw PL strongly by a factor of 60 and decreased PL. These results show that compared to semiconductor devices, the metal chalcogenides and Vander Waals heterostructures are most promising materials for optically active devices. The coupling strength can be tuned in situ by changing the microcavity length. The fabricated monolayer surface gain geometry of microcavity laser shows a new lasing technology which is multipurpose, flexible of any kind and provides a natural gain material replacement facility in Quantum-dot nanocavity laser. These designs can lead to the development of lasers using 2D heterostructures materials such as valley selective lasers and another kind of lasers for on-chip photonic devices.

**REFERENCES :**

- [1] Bryan Ellis, Marie, A. M., Gary Shambat, Tomas Sarmiento, James Harris, Eugene, E. H., and Jelena Vučković. (2011). Ultralow-threshold electrically pumped quantum-dot photonic-crystal nanocavity laser, *Nature Photonics*. 5, 297–300.
- [2] Pallab Bhattacharya, Thomas Frost, Saniya Deshpande, Md ZunaidBaten, Arnab Hazari, and Ayan Das. (2014). Room Temperature Electrically Injected Polariton Laser, *Phys. Rev. Lett.* 112, 236802.
- [3] Imamoglu, A., Ram, R. J., Pau, S. & Yamamoto, Y. (1996). Nonequilibrium condensates and lasers without inversion: Exciton-polariton lasers, *Phys. Rev. A* 53, 4250. DOI: <https://doi.org/10.1103/PhysRevA.53.4250>.
- [4] Kasprzak, J., Richard, M., Kundermann, S., Baas, A., Jeambrun, P., Keeling, JM., Marchetti, FM., Szymańska, MH., André, R., Staehli, JL., Savona, V., Littlewood, PB., Deveaud, B., Dang le, S. (2006). Bose-Einstein condensation of exciton polaritons, *Nature*, 443, 409–414.
- [5] Christopoulos, S., BaldassarriHöger von Högersthal, G., Grundy, A. J. D., Lagoudakis, P. G., Kavokin, A. V., Baumberg, J. J., Christmann, G., Butté, R., Feltin, E., Carlin, J.-F., and Grandjean, N. (2008). Room-Temperature Polariton Lasing in Semiconductor Microcavities, *Phys. Rev. Lett.* 98, 126405. DOI: <https://doi.org/10.1103/PhysRevLett98.126405>.
- [6] Tsintzos, S. I., Pelekanos, N. T., Konstantinidis, G., Hatzopoulos, Z., and Savvidis, P. G. (2008). *Nature*, 453, 372–375.
- [7] Novoselov, K. S., Jiang, D., Schedin, F., Booth, T. J., Khotkevich, V. V., Morozov, S. V., and Geim, A. K. (2005). Two-dimensional atomic crystals, *Proc. Nat. Acad. Sci. USA* 102, 10451–10453.
- [8] Wang, Q. H., Kalantar-Zadeh, K., Kis, A., Coleman, J. N., and Strano, M. S. (2012). Electronics and optoelectronics of two-dimensional transition metal dichalcogenides, *Nat. Nanotechnol.* 7, 699–712.
- [9] Mak, K., Lee, C., Hone, J., Shan, J., and Heinz, T. (2010). Atomically thin MoS<sub>2</sub>: a new direct-gap semiconductor, *Phys. Rev. Lett.* 105, 2–5.
- [10] Dufferwiel, S., Schwarz, S., Withers, F., Trichet, A. A. P., Li, F., Sich, M., Del Pozo-Zamudio, O., Clark, C., Nalitov, A., Solnyshkov, D. D., Malpuech, G., Novoselov, K.S., Smith, J. M., Skolnick, M. S., Krizhanovskii, D. N., and Tartakovskii, A. I. (2015). Exciton-polaritons in van der Waals heterostructures embedded in tunable microcavities, *Nature Communications*, 6(8579), 1-7. DOI: 10.1038/ncomms9579.
- [11] Weisbuch, C., Nishioka, M., Ishikawa, A., and Arakawa, Y. (1992). Observation of the coupled exciton-photon mode splitting in a semiconductor quantum microcavity, *Phys. Rev Lett.* 69, 3314–3317.
- [12] Bhattacharya, P., Xiao, B., Das, A., Bhowmick, S., and Heo, J. (2013). Solid State Electrically Injected Exciton-Polariton Laser, *Phys. Rev. Lett.* 110, 206403.
- [13] Christian Schneider, Arash Rahimi-Iman, Na Young Kim, Julian Fischer, Ivan Savenko, G., Matthias Amthor, Matthias Lerner, Adriana Wolf, Lukas Worschech, Vladimir Kulakovskii, D., Ivan Shelykh, A., Martin Kamp, Stephan Reitzenstein, Alfred Forchel, Yoshihisa Yamamoto, and Sven Höfling. (2013). An electrically pumped polariton laser, *Nature*, 497, 348–352.
- [14] Md ZunaidBaten, Pallab Bhattacharya, Thomas Frost, Saniya Deshpande, Ayan Das, Dimitri Lubyshev, Joel Fastenau, M., and Amy Liu, W. K. (2014). GaAs-based high temperature electrically pumped polariton laser, *Appl. Phys. Lett.*, 104, 231119.

- [15] Sala, V. G., Marsault, F., Wouters, M., Galopin, E., Sagnes, I., Lemaître, A., Bloch, J., and Amo, A.. (2016). Stochastic precession of the polarization in a polariton laser, *Phys.Rev. B*, *93*, 115313.
- [16] Kasprzak, J., Richard, M., Kundermann, S., Baas, A., Jeambrun, P., Keeling, JM, Marchetti, FM, Szymańska, MH, André, R., Staehli, JL, Savona, V., Littlewood, PB, Deveaud, B., Dang le, S. (2006). Bose–Einstein condensation of exciton polaritons, *Nature*, *443*, 409–414.
- [17] Christopoulos, S., BaldassarriHöger von Högersthal, G., Grundy, A. J. D., Lagoudakis, P. G., Kavokin, A. V., Baumberg, J. J., Christmann, G., Butté, R., Feltin, E., Carlin, J.-F., and Grandjean, N. (2007). Room-Temperature Polariton Lasing in SemiconductorMicrocavities, *Phys. Rev. Lett.*, *98*, 126405.
- [18] Christmann, G., Butté, R., Feltin, E., Carlin, J.-F., and Grandjean, N. (2008). Room-temperaturepolariton lasing in a GaN/AlGaN multiple quantum well microcavity, *Appl. Phys. Lett.*, *93*, 051102.
- [19] Ayan Das, JunseokHeo, Marc Jankowski, Wei Guo, Lei Zhang, Hui Deng, and Pallab Bhattacharya. (2011). Room Temperature Ultralow ThresholdGaN Nanowire Polariton Laser, *Phys. Rev. Lett.*, *107*, 066405.
- [20] Pallab Bhattacharya, Thomas Frost, Saniya Deshpande, Md ZunaidBaten, Arnab Hazari, and Ayan Das. (2014). Room Temperature Electrically Injected Polariton Laser, *Phys.Rev. Lett.*, *112*, 236802.
- [21] Lai, Y.-Y., Lan, Y.-P., and Lu, T. -C. (2013). Strong light-matter interaction in ZnOmicrocavities, *Light Sci. Appl.*, *2*, e76.
- [22] Feng Li, Orosz, L., Kamoun, O., Bouchoule, S., Brimont, C., Disseix, P., Guillet, T., Lafosse, X., Leroux, M., Leymarie, J., Mexis, M., Mihailovic, M., Patriarche, G., Réveret, F., Solnyshkov, D., Zuniga-Perez, J., and Malpuech, G. (2013). From Excitonic to Photonic Polariton Condensate in a ZnO-BasedMicrocavity, *Phys. Rev. Lett.*, *110*, 196406.
- [23] Bejtka, K., Réveret, F., Martin, R. W., Edwards, P. R., Vasson, A., Leymarie, J., Sellers, I. R., Duboz, J. Y., Leroux, M., and Semond, F. (2008). Strong light-matter coupling in ultrathin double dielectric mirror GaNmicrocavities, *Appl. Phys. Lett.*, *92*, 241105.
- [24] Christmanna, G., Simeonov, D., Butté, R., Feltin, E., Carlin, J.-F., and Grandjean, N. (2006). Impact of disorder on high-quality factor III-V nitridemicrocavities, *Appl. Phys. Lett.*, *89*, 261101.
- [25] Jayaprakash, R., Kalaitzakis, F. G., Christmann, G., Tsagaraki, K., Hocevar, M., Gayral, B., Monroy,E., and Pelekanos, N. T. (2017). Ultra-low threshold polariton lasing at roomtemperature in a GaN membrane microcavity with a zero-dimensional trap,*Nature Communications*, *7*, 5542. DOI:10.1038/s41598-017-06125-y.
- [26] Hu, P.; Wen, Z.; Wang, L.; Tan, P.; Xiao, K. (2012). Synthesis of few-layer GaSe nanosheets for high performance photodetectors, *ACS Nano*, *6*, 5988 –5994.
- [27] Mudd, G. W., Svatek, S. A., Ren, T., Patan, A.,Makarovsky, O., Eaves, L., Beton, P.H., Kovalyuk, Z. D., Lashkarev, G. V.,Kudrynskyi, Z. R., Dmitriev, A. I. (2013).*Adv. Mater.*, *25*, 5714 –5718.
- [28] Koyama, F. (2006). Recent advances of VCSEL photonics, *IEEE J. Lightwave Technol.*, *24* (12), 4502–4513.
- [29] Hennessy, K., Badolato, A., Winger, M., Gerace, D., Atature, M., Gulde, S., Falt, S., Hu, E. L. Imamoglu, A. (2007).*Nature*, *445*, 896.

- [30] Nowak, A. K., Portalupi, S. L., Giesz, V., Gazzano, O., Dal Savio, C., Braun, P.-F., Karrai, K., Arnold, C., Lanco, L., Sagnes, I., Lemaitre, A., and Senellart, P. (2014). Deterministic and electrically tunable bright single-photon source, *Nat. Commun.*, 5, 3240.
- [31] Holonyak, N., Kolbas, R., Dupuis, R. D., Dapkus, P. D. (1980). *IEEE J. Quantum Electron.*, 16, 170–186.
- [32] Gan, X., Gao, Y., Fai Mak, K., Yao, X., Shiue, R. -J., van der Zande, A., Trusheim, M.E., Hatami, F., Heinz, T. F., Hone, J., Englund, D. (2013). Controlling the spontaneous emission rate of monolayer MoS<sub>2</sub> in a photonic crystal nanocavity, *Appl. Phys. Lett.*, 103, 181119.
- [33] Ross, J. S., Ghimire, N. J., Yan, J., Mandrus, D. G., Yao, W., Hatami, F., Vuckovic, J., Majumdar, A., and Xu, X. (2014). *2D Mater.*, 1, 011001.
- [34] Dolan, P. R., Hughes, G. M., Grazioso, F., Patton, B. R., and Smith, J. M. (2010). *Opt. Lett.*, 35, 3556-8.
- [35] Barbour, R. J., Dalgarno, P. A., Curran, A., Nowak, K. M., Baker, H. J., Hall, D. R., Stoltz, N. G., Petroff, P. M., and Warburton, R. J. (2011). *J. Appl. Phys.*, 110, 053107.
- [36] Dufferwiel, S., Fras, F., Trichet, A., Walker, P. M., Li, F., Giriunas, L., Makhonin, M.N., Wilson, L. R., Smith, J. M., Clarke, E., Skolnick, M. S., and Krizhanovskii, D. N. (2014). *Appl. Phys. Lett.*, 104, 192107.
- [37] Lukas Greuter, Sebastian Starosielec, Daniel Najer, Arne Ludwig, Luc Duempelmann, Dominik Rohner, and Richard Warburton, J. (2014). *Appl. Phys. Lett.*, 105, 121105. DOI: 10.1063/1.4896415.
- [38] Schwarz, S., Dufferwiel, S., Walker, P. M., Withers, F., Trichet, A. A. P., Sich, M., Li, F., Chekhovich, E. A., Borisenko, D. N., Kolesnikov, N. N., Novoselov, K. S., Skolnick, M. S., Smith, J. M., Krizhanovskii, D. N., and Tartakovskii, A. I. (2014). Two-Dimensional Metal – Chalcogenide Films in Tunable Optical Microcavities, *Nano Lett.*, 14, 7003 –7008. dx.doi.org/10.1021/nl503312x.
- [39] Humberto Gutiérrez, R., Nestor Perea-López, Ana Laura Elías, Ayse Berkdemir, Bei Wang, Ruitao Lv, Florentino López-Urías, Vincent Crespi, H., Humberto Terrones, and Mauricio Terrones. (2013). Extraordinary Room-Temperature Photoluminescence in Triangular WS<sub>2</sub> Monolayers, *Nano Letters*, 13, 3447–3454.
- [40] Rong, Y., Fan, Y., Leen Koh, A., Robertson, AW, He, K., Wang, S., Tan, H., Sinclair R., Warner, JH. (2014). Controlling sulphur precursor addition for large single crystal domains of WS<sub>2</sub>, *Nanoscale*, 6, 12096–12103.
- [41] Jiang, J.-H., and John, S. (2014). Photonic Architectures for Equilibrium High-Temperature Bose-Einstein Condensation in Dichalcogenide Monolayers, *Scientific Reports* 4, 7432.
- [42] Bohua Chen, Xiaoyan Zhang, Kan Wu, Hao Wang, Jun Wang, and Jianping Chen. (2015). Q-switched fibre laser based on transition metal dichalcogenides MoS<sub>2</sub>, MoSe<sub>2</sub>, WS<sub>2</sub>, and WSe<sub>2</sub>, *Optics Express*, 23, 26723-26737.
- [43] Vasilevskiy, M. I., Santiago-Pérez, D. G., Trallero-Giner, C., Peres, N. M. R., and Kavokin, A. (2015). Exciton polaritons in two-dimensional dichalcogenide layers placed in a planar microcavity: Tunable interaction between two Bose-Einstein condensates, *Physical Review B*, 92, 245435.
- [44] Lu, J., Liu, H., Tok, E. S., and Sow, C.-H. (2016). Interactions between lasers and two-dimensional transition metal dichalcogenide, *Chem Soc Rev.*, 45(9), 2494-515. doi: 10.1039/c5cs00553a.
- [45] Zhu, B., Chen, X., and Cui, X. (2015). Exciton Binding Energy of Monolayer WS<sub>2</sub>, *Scientific Reports*, 5, 9218.

- [46] Zhao, W., Ghorannevis, Z., Chu, L., Toh, M., Kloc, C., Tan, PH, Eda, G. (2013). Evolution of Electronic Structure in Atomically Thin Sheets of WS<sub>2</sub> and WSe<sub>2</sub>. *ACS Nano*, 7, 791–797.
- [47] Xu, X., Yao, W., Xiao, D., and Heinz, T. F. (2014). Spin and pseudospins in layered transitionmetal dichalcogenides, *Nature Physics*, 10, 343–350.
- [48] Scrace, T., Tsai, Y., Barman, B., Schweidenback, L, Petrou, A., Kioseoglou, G., Ozfidan, I., Korkusinski, M., andHawrylak, P. (2015). Magnetoluminescence and valley polarized state of a two-dimensionalelectron gas in WS<sub>2</sub> monolayers, *Nature Nanotechnology* 10, 603–607.
- [49] Matin Amani, Der-Hsien Lien, Daisuke Kiriya, Jun Xiao, Angelica Azcatl, Jiyoung Noh, Surabhi Madhvapathy, R., Rafik Addou, Santosh, KC, Madan Dubey, Kyeongjae Cho, Robert Wallace, M., Si-Chen Lee, Jr-Hau He, Joel Ager III, W., Xiang Zhang, Eli Yablonovitch, Ali Javey. (2015). Near-unity photoluminescence quantum yield in MoS<sub>2</sub>, *Science*, 350,1065–1068.
- [50] Xiaoze Liu, Tal Galfsky, Zheng Sun, Fengnian Xia, Erh-chen Lin, Yi-Hsien Lee, Stéphane Kéna-Cohen, and Vinod Menon, M. (2015). Strong light-matter coupling in two-dimensional atomic crystals, *NaturePhotonics*, 9, 30–34.
- [51] Schwarz, S., Dufferwiel, S., Walker, P. M., Withers, F., Trichet, A. A. P., Sich, M., Li, F., Chekhovich, E. A., Borisenko, D. N., Kolesnikov, N. N.,Novoselov, K. S., Skolnick, M. S., Smith, J. M., Krizhanovskii, D. N., and Tartakovskii, A. I. (2014). Two-Dimensional Metal-Chalcogenide Films in Tunable OpticalMicrocavities, *Nano Letters*, 14, 7003–7008.
- [52] Dufferwiel, S., Schwarz, S., Withers, F., Trichet, AA, Li, F., Sich, M., Del Pozo-Zamudio, O., Clark, C., Nalitov, A., Solnyshkov, DD, Malpuech, G., Novoselov, KS, Smith, JM, Skolnick, MS, Krizhanovskii, DN, and Tartakovskii, AI. (2015). Exciton-polaritons in van der Waals heterostructures embedded intunable microcavities, *Nature Communications*, 6, 8579.
- [53] Flatten, L. C., He, Z., Coles, D. M., Trichet, A. A. P., Powell,A. W., Taylor, R. A., Warner,J. H., Smith, J. M. (2016). Room-temperature exciton-polaritons with two-dimensionalWS<sub>2</sub>, *Scientific Reports*, nature, 6, 33134. DOI: 10.1038/srep33134,2016
- [54] Oulton, RF., Sorger, VJ., Zentgraf, T., Ma, RM., Gladden, C., Dai, L., Bartal, G., and Zhang, X. (2009). Plasmon lasers at deep subwavelength scale, *Nature*, 461,629–632.
- [55] Lu, YJ., Kim, J., Chen, HY., Wu, C., Dabidian, N., Sanders, CE., Wang, CY., Lu, MY., Li, BH., Qiu, X., Chang, WH., Chen, LJ., Shvets, G., Shih, CK., Gwo, S. (2012). Plasmonic nanolaser using epitaxially grown silver film, *Science*, 337,450–453.
- [56] Painter, O., Lee, R. K., Scherer, A., Yariv, A., O'Brien, J. D., Dapkus, P. D., Kim, I. (1999). Two-dimensional photonic band-gap defect mode laser, *Science*, 284,1819–1821.
- [57] Khajavikhan, M., Simic, A., Katz, M., Lee, J. H., Slutsky, B., Mizrahi, A., Lomakin, V., and Fainman, Y. (2012).Thresholdless nanoscale coaxial lasers, *Nature*, 482, 204–207.
- [58] Martin Hill, T., Yok-Siang Oei, Barry Smalbrugge, Youcai Zhu, Tjibbe de Vries, Peter van Veldhoven, J., Frank van Otten, W. M., Tom Eijkemans, J., JarosławTurkiewicz, P., Huug de Waardt, Erik Jan Geluk, Soon-Hong Kwon, Yong-Hee Lee, Richard Nötzel, and Meint Smit, K. (2007). Lasing in metallic-coated nanocavities, *Nature Photon*, 1, 589–594.
- [59] Strauf, S., Hennessy, K., Rakher, M. T., Choi, Y.-S., Badolato, A., Andreani, L. C., Hu, E. L., Petroff, P. M., and Bouwmeester, D. (2006). Self-tuned quantum dot gain in photonic crystal lasers, *Phys. Rev.Lett.*, 96, 127404.
- [60] Strauf, S., and Jahnke, F. (2011). Single quantum dot nanolaser, *Laser Photon Rev.*, 5,607–633.
- [61] Bryan Ellis, Marie Mayer, A., Gary Shambat, Tomas Sarmiento, James Harris, Eugene Haller, E., and Jelena Vučković. (2011). Ultralow-threshold electrically pumped quantum-dot photoniccrystalnanocavity laser, *Nature Photon*, 5, 297–300.

- [62] Mak, K.F., Lee, C., Hone, J., Shan, J., and Heinz, T.F. (2010). Atomically thin  $\text{MoS}_2$ : a new direct-gap semiconductor, *Phys. Rev. Lett.*, *105*, 136805.
- [63] Andrea Splendiani, Liang Sun, Yuanbo Zhang, Tianshu Li, Jonghwan Kim, Chi-Yung Chim, Giulia Galli, and Feng Wang. (2010). Emerging photoluminescence in monolayer  $\text{MoS}_2$ . *Nano Lett.*, *10*, 1271–1275.
- [64] Mak, K. F., He, K., Lee, C., Lee, G. H., Hone, J., Heinz, T. F., Shan, J. (2013). Tightly bound trions in monolayer  $\text{MoS}_2$ , *Nature Mater.*, *12*, 207–211.
- [65] Jason Ross, S., Sanfeng Wu, Hongyi Yu, Nirmal Ghimire, J., Aaron Jones, M., Grant Aivazian, Jiaqiang Yan, David Mandrus, G., Di Xiao, Wang Yao, and Xiaodong Xu. (2013). Electrical control of neutral and charged excitons in a monolayer semiconductor, *Nature Commun.*, *4*, 1474.
- [66] Aaron Jones, M., Hongyi Yu, Nirmal Ghimire, J., Sanfeng Wu, Grant Aivazian, Jason Ross, S., Bo Zhao, Jiaqiang Yan, David Mandrus, G., Di Xiao, Wang Yao, Xiaodong Xu. (2013). Optical generation of excitonic valley coherence in monolayer  $\text{WSe}_2$ , *Nature Nanotechnol.*, *8*, 634–638.
- [67] Xiao, D., Liu, G.-B., Feng, W., Xu, X., and Yao, W. (2012). Coupled spin and valley physics in monolayers of  $\text{MoS}_2$  and other group-VI dichalcogenides, *Phys. Rev. Lett.*, *108*, 196802.
- [68] Xu, X., Yao, W., Xiao, D., and Heinz, T. F. (2014). Spin and pseudospins in layered transition metal dichalcogenides, *Nature Phys.*, *10*, 343–350.
- [69] Radisavljevic, B., and Kis, A. (2013). Mobility engineering and a metal-insulator transition in monolayer  $\text{MoS}_2$ , *Nature Mater.*, *12*, 815–820.
- [70] R. S. Sundaram, M. Engel, A. Lombardo, R. Krupke, A. C. Ferrari, Ph. Avouris, and M. Steiner. (2013). Electroluminescence in single layer  $\text{MoS}_2$ , *Nano Lett.*, *13*, 1416–1421.
- [71] Baugher, B. W. H., Churchill, H. O. H., Yang, Y., and Jarillo-Herrero, P. (2014). Optoelectronic devices based on electrically tunable p-n diodes in a monolayer dichalcogenide, *Nature Nanotechnol.*, *9*, 262–267.
- [72] Ross, J. S., Klement, P., Jones, A. M., Ghimire, N. J., Yan, J., Mandrus, D. G., Taniguchi, T., Watanabe, K., Kitamura, K., Yao, W., Cobden, D. H., Xu, X. (2014). Electrically tunable excitonic light-emitting diodes based on monolayer  $\text{WSe}_2$  p-n junctions, *Nature Nanotechnol.*, *9*, 268–272.
- [73] Pospischil, A., Furchi, M. M., and Mueller, T. (2014). Solar-energy conversion and light emission in an atomic monolayer p-n diode. *Nature Nanotechnol.*, *9*, 257–261.
- [74] Lopez-Sanchez, O., Lembke, D., Kayci, M., Radenovic, A., and Kis, A. (2013). Ultrasensitive photodetectors based on monolayer  $\text{MoS}_2$ , *Nature Nanotechnol.*, *8*, 497–501.
- [75] Sanfeng Wu, Sonia Buckley, John R Schaibley, Liefeng Feng, Jiaqiang Yan, David G Mandrus, Fariba Hatami, Wang Yao, Jelena Vučković, and Arka Majumdar. (2015). Monolayer semiconductor nanocavity lasers with ultralow thresholds, *Nature*, *520* (7545), 69. doi:10.1038/nature14290.

\*\*\*\*\*